Analysis of the beam test data collected at CERN Proton Synchrotron Facility

Jim Bloemkolk

Supervisors:
dr. ir. G J Nooren
dr. E Rocco

Utrecht University.

Department of Physics
Institute of Subatomic Physics

January 14, 2015

Abstract

In this bachelor research project the trigger system of the FOCAL prototype detector is studied in detail and the data, gathered at the Proton Synchrotron beam test (September 2014), is analysed for data quality checks and the study of hadronic shower production for both pions and protons. During the beam test a flat cable, carrying trigger information, was damaged. This data is reconstructed to make analysis possible. There also were unknown patterns found in the trigger data that was studied in more detail in an attempt to increase the efficiency of the detector. The study of hadronic showers does not result in any conclusions because the expected shower characteristics are not found in the data. Also some data quality issues remain unresolved and prevent proper study of the hadronic showers.

Contents

Chapter 1

Introduction

This bachelor research is done at the FOCAL (FOrward CALorimeter) group, working at the Institute of Subatomic Physic at the Utrecht University. This group is working on a prototype calorimeter using high density wolfram absorber material and high resolution silicon detector chips. This prototype is under development to test the usefulness of these kind of detectors as part of the next scheduled large scale upgrade of ALICE (A Large Ion Colider Experiment) at CERN.

The contribution of this research is focused on the beam test at CERN done in September 2014. In chapter 6, the data gathered during these measurement is analysed and checked for anomalies to make sure the data quality is sufficient for further use in improving the FOCAL design. Also, in chapter 5 the trigger system is analysed in detail and a problem that prevents proper analysis is fixed. During the trigger system analysis unexplained "ghost" triggers are found and addressed.

Chapter 2

Theoretical background

2.1 Particles through matter

When particles traverses matter they interact in various ways depending on the particle and the material. In the beam test done for this thesis the particles that enter the detector are mainly electrons, protons, pions and muons. These particles behave differently due to their different interaction lengths and varying shower characteristics.

2.1.1 Light charged particles

When light charged particles, like electrons, move through a medium they can interact with it in multiple ways. The two main factors of energy loss are "radiative energy loss" and "collisional energy loss". [1]

Radiative loss is caused by the deflection of the charged particles by the nuclei in the material. The particle moving through the matter experiences the electric fields of the atoms in this matter. The positively charged nuclei attract the light charged particles, accelerating them by changing its direction. This acceleration of charge gives off something that is called "Bremsstrahlung" [2]. The energy of the photon that is ejected depends on the amount of deflection of the electron. Because an atom is usually neutral, this effect becomes very small for larger distances. For shorter distances, the electron will feel more of the nucleus' charge and therefore deflect more. This effect is called screening, because the electron cloud orbiting the nucleus will screen the nucleus' charge for the deflected electron. It is also possible for a direct stop of the electron. This happens more often in materials with a lot of positive charge in the nucleus. When this happens all the kinetic energy of the electron will go into the produced photon. An additional effect of this deflecting of the electron is that it doesn't travel in a straight line, but takes a longer route. This means that the traveled distance can be different from the penetration depth.

Collisional energy loss is when the electron interacts, not with the nucleus, but with the orbital electrons of the medium. The word "collisional" suggests that the electrons must come into direct contact, but because the long range nature of the electromagnetic force this is not the case. The maximum energy loss of the electron, in a head-on collision, is its total kinetic energy. Because the collision is between two equally massive particles (electrons) the opening angle can be greater than that of a heavy particle interacting with orbital electrons. When the two electrons interact, the orbital electron can gain energy and excite to a higher energy level. When this electron falls back to its original energy level it ejects a photon.

2.1.2 Heavy charged particles

The heavy charged particles that enter the detector are the protons, pions and muons. The primary stopping power is that of the orbital electrons in the medium. The heavy charged particles interact with these electrons and can excite them to higher energies. If there is enough momentum transfer the atoms can be ionized. Because the incoming particle is much heavier than the orbital electrons it interacts with, the path of these heavy charged particles is, unlike the light charged particles, more or less a straight line. [3] The energy loss due to the ionisation of the orbital electron in the vicinity of the heavy charged particle is given by the Bethe-Bloch formula:

$$-\left\langle \frac{dE}{dx} \right\rangle \propto -\frac{n}{\beta^2}\left(\ln\left(\text{const}\cdot\beta^2\gamma^2\right)-\beta^2\right). \tag{2.1}$$

In this formula n is the electron density of the medium and β is proportional to the velocity of the particle.

There is also a chance that the proton or pion has a inelastic collision with the atoms nucleus. This happens only at collisions with high energy transfer, typically where about half of the available energy is consumed. The remaining kinetic energy goes into forward-going particles with high velocity. The secondary particles created are typically pions and nuclei. The neutral pions (π_0) that are created decay into two photons after interacting with a nucleus ($\pi \rightarrow \gamma\gamma$). The fraction of π_0 is about

$$0.10\ln\left(E\,\text{in GeV}\right).[4] \tag{2.2}$$

Another sizable fraction of the total available kinetic energy is converted into excitations of the nucleus or ejection of parts of the nucleus. If the collision ejects a neutron this will not be detected by the detector. [5]

2.1.3 Photons

When a photon goes through matter in can interact with different mechanisms. In the lower energy regions of photons, like visible light an ultraviolet light, the photon can be absorbed by an orbital electron that then excites its energy state. When the energy of the photon becomes too large (higher energy ultraviolet light and X-rays) the electron that absorbs the photon will gain too much energy to be bounded by the atom anymore. When this happens the atom will be ionized (figure 2.1 (b)) and the electron will be ejected. When the recoil electron is ejected at an angle from the incoming photon, another photon will be emitted in the process to conserve momentum. This process is called Compton scattering (figure 2.1 (b)). [6]

With high enough energy photons (X-rays) it is also possible for the photon to create an electron-positron pair (figure 2.1 (c)). This process need the electric field of an atom to preserve momentum and provide a rest-frame for the process. The photon must have at least the energy of the added rest masses of the electron and positron, so 1.022 MeV. For even higher energy photons it is possible to create different particle anti-particle pairs, but at the energies studied in this thesis this process does not occur. [7]

2.1.4 Heavy neutral particles

Heavy neutral particles don't come from the beam, but can be created in a collision. If it is a neutron, the detector won't be able to detect the particle and therefor underestimates the energy

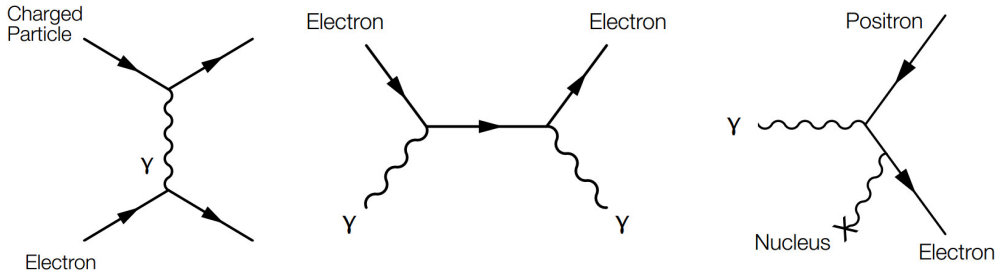

(a) Ionisation **(b)** Compton scattering **(c)** Pair production

Figure 2.1: The three mechanisms of photon interactions with matter.

of the incoming particle. Neutral pions will decay quickly into two photons that can undergo pair production ($\pi \rightarrow \gamma\gamma \rightarrow 2 \cdot e + 2 \cdot p$). The charged particles produced in this process are detectable by the detector.

2.2 Particle showers

When a high energy particle enters the detector it can undergo a series of interactions (explained before) that causes more particles to be created. This process is called "showering" and makes it possible to measure the energy of the incoming particle in the FOCAL prototype. There are two main categories of showers: the electromagnetic shower and the hadronic shower.

2.2.1 Electromagnetic showers

The electromagnetic shower is a particle shower with electrons, positrons and photons. An incoming electron is deflected by the charge of a nucleus. This accelerations causes a bremsstrahlungs photon to be produced. The photon then can undergo pair-production with a nucleus to produce an electron and a positron. These two particles are again deflected by surrounding nuclei and produce a photon. This process keeps on going till the photons that are produced no longer have enough energy for pair prodcution. The shower also looses energy due to all the other interaction processes shown above, but they don't produce more particles to be detected.

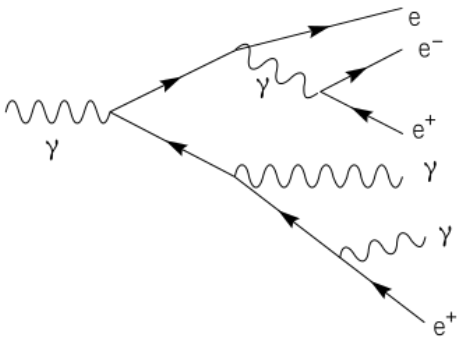

Figure 2.2: Progression of an electromagnetic shower. [8]

2.2.2 Hadronic showers

The hadronic shower is more complex than the electromagnetic shower. The electromagnetic showers are studied extensively and can be analytically modelled with quantum electrodynamics, but the hadronic showers are influenced by the strong nuclear force. Adding to that, the electromangetic showers have steady and sub-nanosecond time scales but a hadronic showers has different interaction mechanisms with different time scales. Nuclear excitations can have half-life times of microseconds. Although there are so many variables in the hadronic shower progressions that are complex and not fully understood (analytically), something can be said about the shower parameters such as shower maximum, depth and radial containment. The shower maximum is approximately given by:

$$L_{max} \approx \lambda \left(0.6 \ln(E \text{ in } GeV - 0.2)\right), \tag{2.3}$$

where λ is the interaction length. The interaction length depends on the material the shower is forming in and is normally larger for denser materials with heavy nuclei. The longitudinal containment (of 95%), the shower depth, is approximately:

$$L_{containment} \approx L_{max} + 4\lambda (E \text{ in } GeV)^{0.15}.[4] \tag{2.4}$$

At last the radial containment (of 95%) can be approcimated with:

$$R_{containment} \approx \lambda.[4] \tag{2.5}$$

These parameters can be used to make a prediction for the showers produced in the FOCAL protype.

Chapter 3

Experimental setup

3.1 Accelerator and the beamline

This thesis will be restricted to the Proton synchrotron beam test, as this has been used for the data that the majority of this thesis covers.

The Proton Synchrotron (or PS for short) is the first major accelerator build at the CERN institute and it is still used to accelerate protons and heavy ions to up to 25 GeV. The protons are fed into the ring by the Proton synchrotron Booster and when heavy ions are used they are delivered by the Low Energy Ion Ring (or LEIR). The PS accelerated its first protons on 24 November 1959 and is still used to feed particles into the Super Proton Synchrotron (SPS) and the Antiproton Decelerator (AD). Besides accelerating particles for other stages in the CERN Accelerator Complex the PS also ejects so called 'spills' into the East Hall, where the experiment this thesis covers was situated. The FOCAL prototype was set up in the T9 test area. [9]

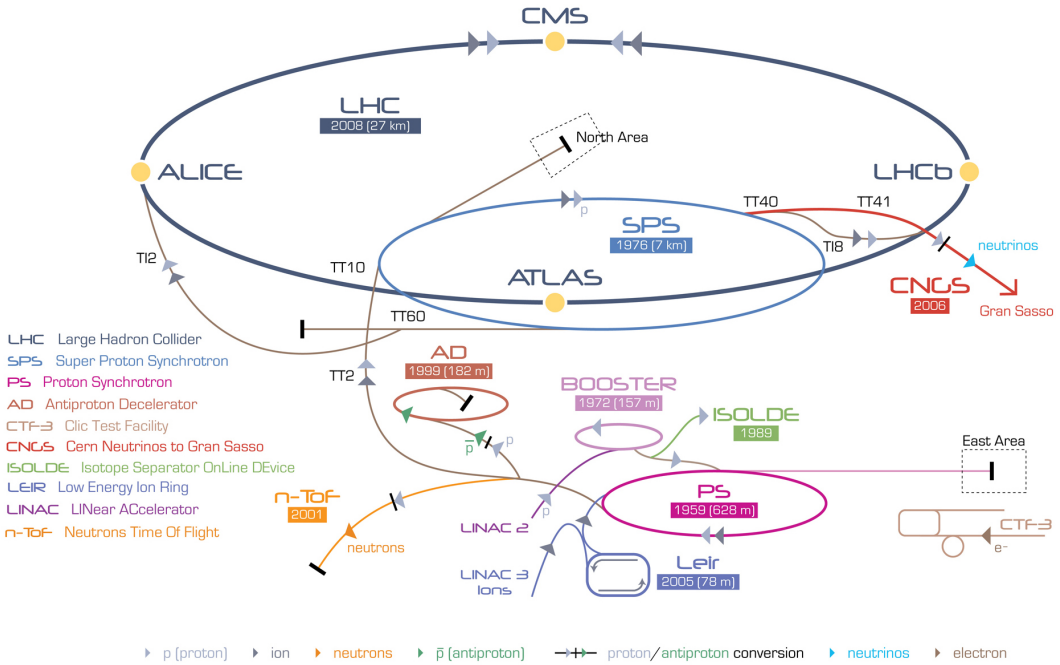

Figure 3.1: The CERN Accelerator Complex. This diagram shows the different accelerators and destinations of the particles.

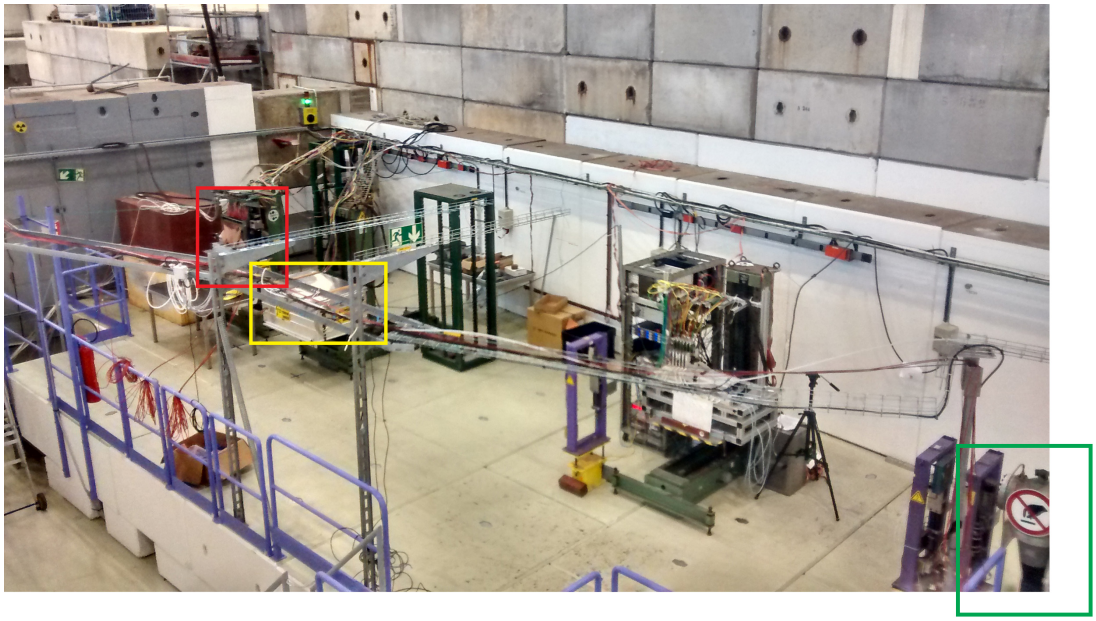

Figure 3.2: T9 test area photographed from an overview point. Highlighted with the different colors are: FOCAL detector (red), Straw Man detector (yellow) and one of the Cherenkov detectors (green).

3.1.1 Beam composition

As measured by other research groups, the beam composition of the East-Hall T9 test area is shown in figure 3.3. The negative momentum beam is primarily composed of electrons and pions at the lower momenta and only pions at the higher. The positive momentum beam is primarily composed of positrons and pions at the lower momenta and protons and pions at the higher momenta.

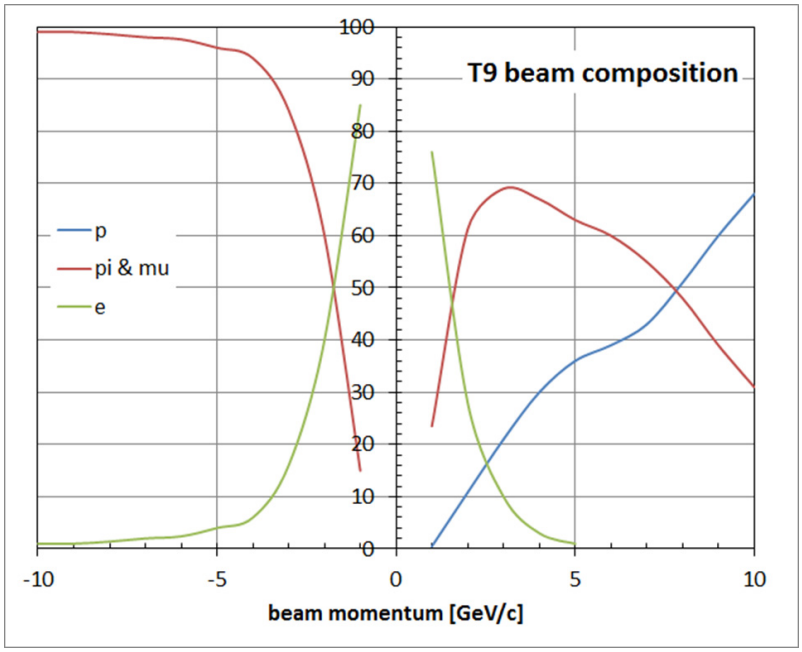

Figure 3.3: Measured beam composition of the T9 test area. [10]

3.2 The components

Figure 3.4 shows the experimental setup used at the PS beam test. The detector is surrounded by auxiliary detectors: scintillators and Cherenkov detectors. In these plots the extra layers with copper absorption block are also shown. The position of the second Cherenkov detector is shown in figure 3.2, as well as the FOCAL detector position. The scintillators are labelled with letters. Their size and position are found in table 3.1.

Label	Size	Position
F	4 cm^2	Front
P	10 cm^2	
H	1 cm^2	
V	1 cm^2	
B	4 cm^2	Back

Table 3.1: Different scintillators with size and position.

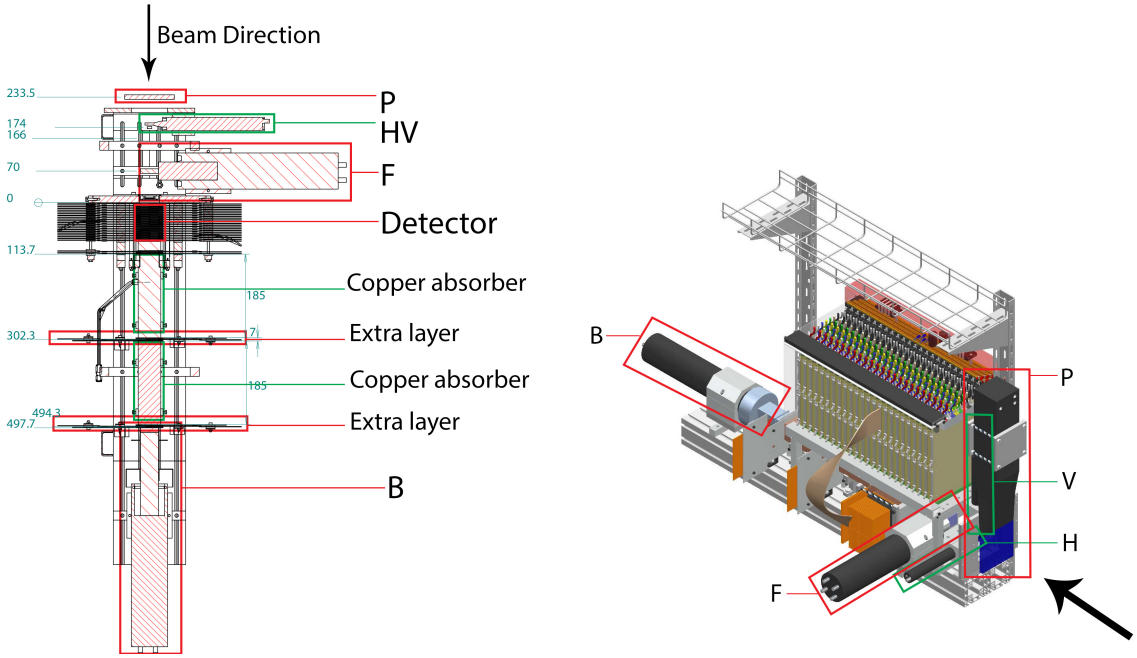

(a) Top view **(b)** 3D view

Figure 3.4: Schematic view of the detector with the important components highlighted. [11]

3.3 Extra layers for hadronic shower

The last two layers of the detector are added to get better hadronic shower containment for pions and protons. As is visible in figure 3.4 (a), the two extra layers had to be taken out of the detector and put behind the copper. This is not because there are not enough detector chips, but because all the channels of the Virtex box (see chapter 4) are occupied. Table 3.2 shows the resulting interaction lengths for both pions and protons in this setup.

Table 3.2: Length of the detector in units of interaction length for protons and pions. (ref Gert Jan)

Up to layer	Radiation lengths	Pion interaction lengths	Proton interaction lengths
23	28	0.9	1.2
24	43	1.9	2.2
25	56	2.9	3.2

Chapter 4

The detector

The setup used for the PS beam test is a combination of different detectors that run in parallel. In this section those detectors their working, settings and calibration are discussed. In this chapter the conclusions and perspectives are discussed.

4.1 FOCAL prototype

The FOCAL prototype is the main detector and the one being studied by the FOCAL group. This detector is a digital electromagnetic sampling calorimeter. 'Digital' because it chips measure only if pixels are on or off, 'electromagnetic' because the chips measure the charge that is accumulated and 'sampling' because active layers (silicon) that detect the charged particles are different from the absorption layers (tungsten) that can be made passive (without electronics). [5]

4.1.1 MAPS chips

The FOCAL detector is a combination of tungsten, a high density absorbing material and silicon MAPS chips. MAPS stand for 'Monolithic Active Pixel Sensors'. In these chips the charge that is deposited by the passing particles (and charge generated by other means) is captured in a n-well. The electrons are being 'guided' to this well by the differently doped layers of silicon. If the collected charge is surpassing the threshold (further discussed in section 4.1.2) the pixel is defined as a 'hit' for that particular read out cycle. The MAPS chips have a resolution of 640x640 and therefore a total of 409600 pixels packed on an area of 19.2x19.2 mm^2. The pixels themselves contain the electronics to capture the charge, but not to measure it. The chips can be read out at a frequency of 160 Hz. The detector has a total of 96 chips in 24 layers of 4 chips per layer. At this time not all chips are working properly or give a signal at all.

Reading out the chips

The chips are not read out in its entirety each cycle, but read out one line at a time. The chips select a line and measure the accumulated charge of each pixel on that line with a different discriminator. The discriminator determines if the charge surpasses its threshold and therefore determining whether the pixel is considered hit or not. This process of selecting the chips line after line is called a "rolling shutter" and makes it possible to use 640 times less discriminators. Due to this rolling shutter not all lines are read out simultaneously, so this has to be accounted for during analysis. The discriminators are attached to four different channels that are used to ship the data out.

4.1.2 Thresholds

When the accumulated charge flows through the discriminator is it compared to a certain threshold. This threshold can be set with two parameters: Vref1 and Vref2. The first controls the sensitivity of the whole chip and the second controls the left-to-right sensitivity. The Vref2 parameter is used to tune the balance of the row (left to right) connected to different discriminators. The different chips can have varying sensitivities, so the tuning of the thresholds is very important to get consistent measurement across the different chips. At the moment of writing there is not yet an automated method of calculating the optimal thresholds. The procedure now is to take background measurements (or "pedestal measurement") and tune the thresholds by eye. A pedestal measurement of tuned chips would look like figure 4.1

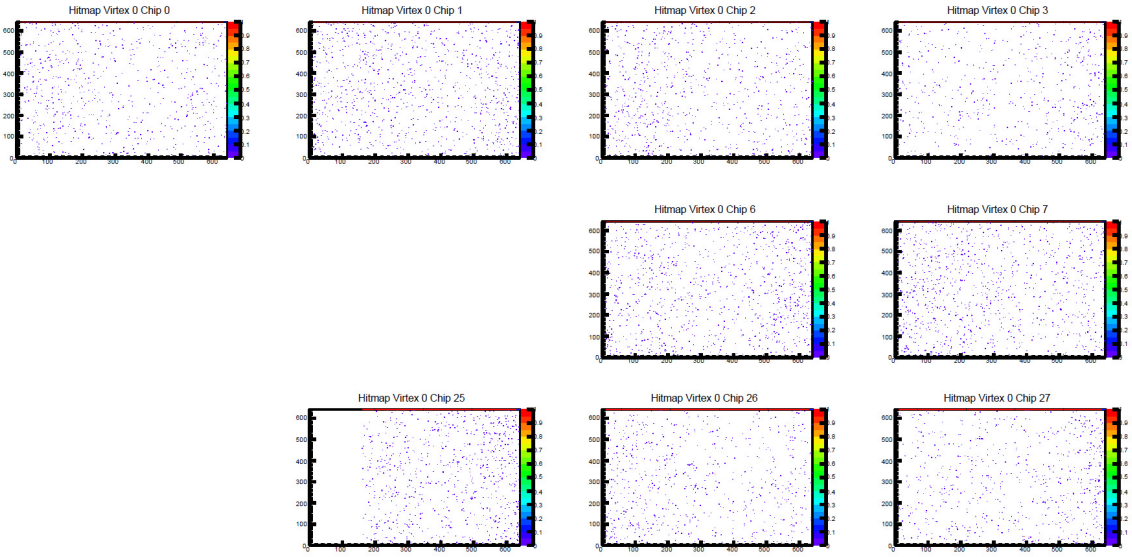

Figure 4.1: Pedestal hit maps of tuned chips.

4.2 Auxiliary detectors

To gain information about particles and to use as triggers (see chapter 5), auxiliary detectors are used. At the PS beam test both scintillators and Cherenkov detectors were used.

4.2.1 Scintillators

Scintillator counters are made out of two components: a piece of scintillating material and a photomultiplier tube. The scintillator material is most commonly a kind of plastic. When a particle enters the scintillating material the orbital electrons in the material get excited. When these electron fall back to their ground state they emit a photon. The direction of this photon is not dependent of the direction of the incoming particle. A part of the photons will be emitted in the direction of the photomultiplier tube. This device has a photo cathode so the photon will easily ionise an electron that, with a high voltage applied, will be multiplied by the photo multiplier tube to a signal that can be used. This process is visualised in figure 4.2.

4.2.2 Cherenkov Detectors

A Cherenkov detector uses the Cherenkov effect to create the photons that afterwards are, like in scintillators, amplified to an electrical signal by a photomultiplier tube. The Cherenkov effect is

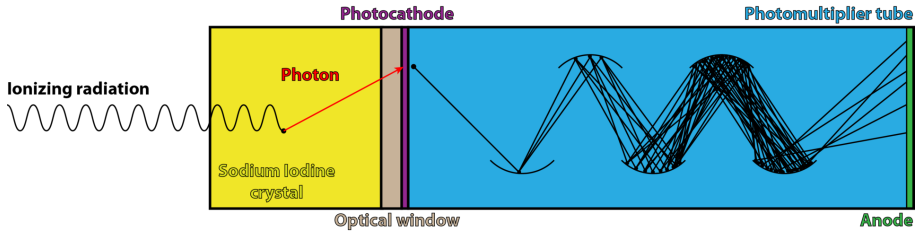

Figure 4.2: Schematic diagram of a scintillator counter. The light that enters the cintillating material is converted to an electron and the photomultiplier tube amplifies this signal. [12]

like a sonic boom for electromagnetic waves. When a particle travels through a medium faster than light travels in that medium it creates an electromagnetic shock wave that can be detected as bluish light in the visible spectrum. When charged particles move through a medium, they disturb the energy levels of the orbital electrons. The electrons get excited and wen they relax again they emit a faint light. If the particle travels faster than the velocity of this light constructive interference will enhance the amplitude of the shock front. The Cherenkov detector can be used to give light at a specific velocity by tuning the pressure of the gas inside the chamber. At the PS beam test the pressure was set at 0.5 bar to differentiate between electron and pions at lower energies and proton and pions at higher energies.[13]

4.2.3 Plateaus of the photomultiplier tubes

Photomultiplier tubes need a high voltage power supply in order to amplify the signal enough to be usable. The voltage on the power supplies can be varied and will give different count rates. To calibrate the tubes it is useful to find a plateau in this count rate. The used voltage is centered on the plateau so the count rate is not effected considerably when the voltage changes slightly. The first attempt to calibrate the P-scintillator with cosmic radiation was not a success as seen in figure 4.3. Even with a lot of data points no plateau is present. It could suggest that there might be a plateau around $1950\,V$, but further measurement was needed to confirm this.

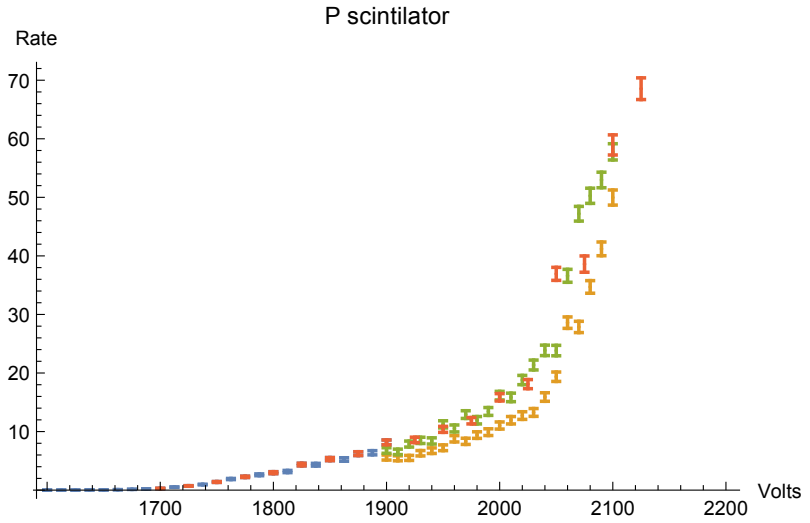

Figure 4.3: First plateau measurement using cosmic radiation.

To better find the plateaus the next step was measuring the count rate of the scintillators in the beam. This gives an increased count rate of a few orders compared to measuring with cosmic

rays. The measured data is plotted in figure 4.4. The used voltages are shown in the graphs. The F- and P-scintillator have well defined plateaus, but there were still problems with the H- and V-scintillator. When the scintillators are put in coincidences (see section 4.3) the noise is reduces to almost nothing. This is why it was decided to stay with the in figure 4.4 chosen voltages.

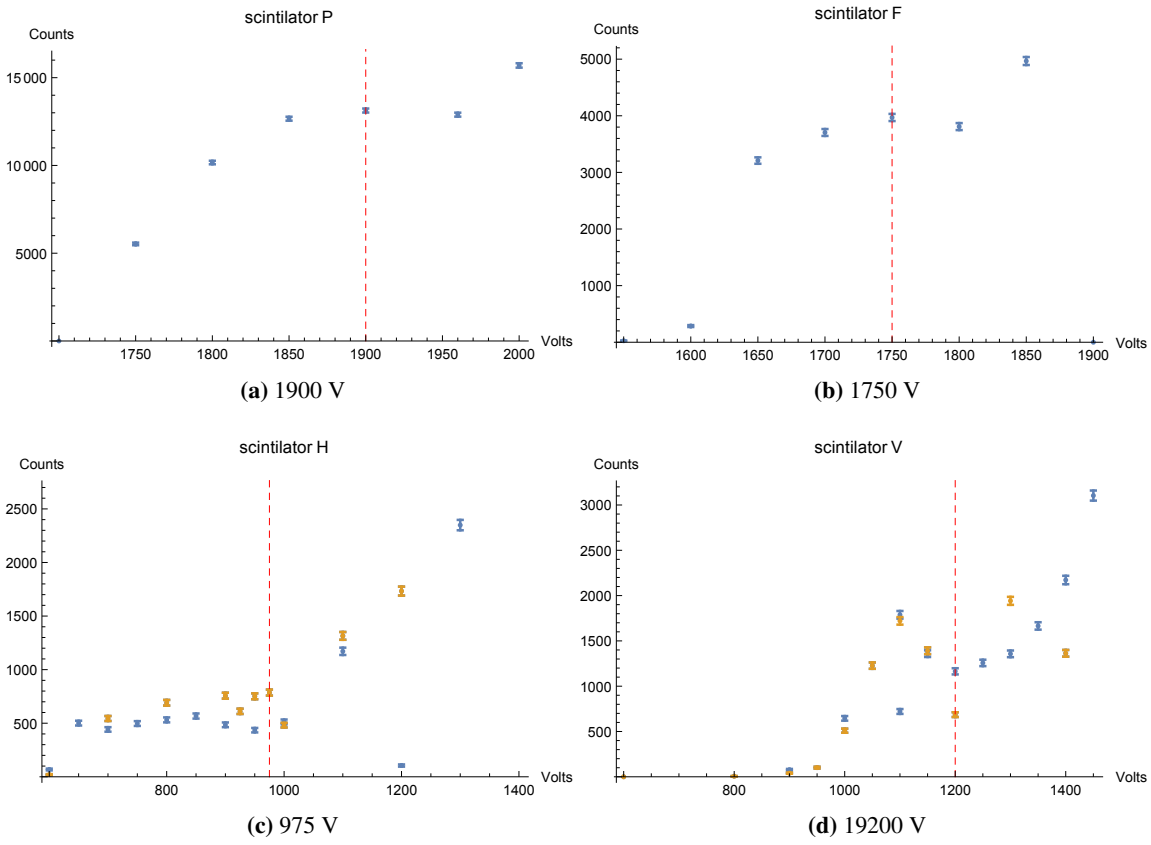

(a) 1900 V **(b)** 1750 V

(c) 975 V **(d)** 19200 V

Figure 4.4: Scintillator plateaus with corresponding voltage used in the PS beam test.

4.3 Trigger logic and particle selection

The photomultiplier tubes of the scintillators and Cherenkov detectors produce a raw signal varying in amplitude and width. This signal is injected into a discriminator that is set to a threshold of -30 mV and produces a NIM-pulse (negative pulse with fast rise time and varying length and amplitude) when this threshold is reached. In the whole logic circuit the NIM or TTL (positive pulse) standards are used.

The discriminators produce digital signals that can be used to make different coincidences with. This means that there are different combinations of triggers made to correspond to different species of particles or give geometric information about the particle that is detected. At the Proton Synchrotron experiment, four different trigger combinations where used at a time.

- PF. This trigger will fire if any particle enters the detector and thus serving as the main trigger.
- BF. This trigger gives information about the penetration depth of the particle. The B scintillator is placed at the back of the detector and is expected to detect no electrons. The

electrons are all absorbed into the calorimeter (as is necessary to measure their energy).

- C_1C_2F. Cherenkov detectors discriminate between masses of particles because all the particles in the beam have the same momentum.

- HVF. This trigger gives only geometric information about the particle detected. Both H and V are small 1 cm scintillators that are placed in the middle of the detector. When this trigger fires the particle has hit the middle of the calorimeter.

- Spill trigger. This signal is delivered by the PS or SPS system and marks the beginning of a spill. This trigger is used to start the data acquisition.

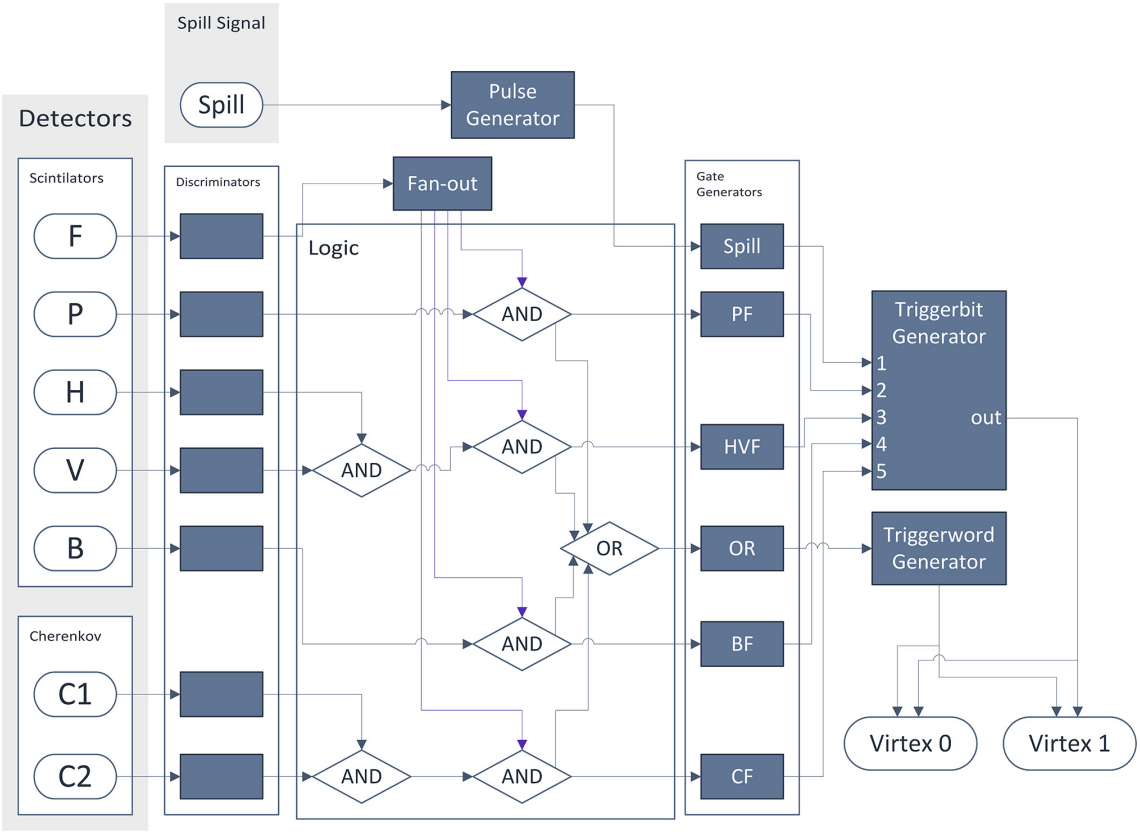

Figure 4.5: The connection diagram of the trigger logic. The discriminators are set to a threshold of -30 mV and a pulse width of 60 ns. The pulse generator pulse width is set at the measuring time per spill: 0.55 s. The spill delay is 10 s. The gate generators make a NIM pulse widt a width of 300ns. Delay boxes are added at appropriate positions in the diagram to make the pulses reach the AND and OR gates at the same time.

4.3.1 Particle selection

With the trigger information from the Cherenkov detectors it is possible to distinguish particles from each other. The Cherenkov chamber's pressure is tuned at 0.5 bar to make it possible to distinguish electrons from pions and muons at negative and lower energies and distinguish between protons and pions/muons at higher positive energies. This is very helpful information that can be used to select data from certain events if you know what particles you want to study.

4.4 Virtex boxes

The Virtex boxes are connected to the electronics in the detector and the trigger logic in the control room. It records this information in its memory (2 Gigabytes) and sends it to the DAQ (Data Acquisition Machine, a powerful workstation used to store and analyse the data). It also provides the possibility to send the proper settings to the chips and perform diagnostics. There are two Virtex boxes used (V0 and V1) that are both connected to half of the chips. Inside the Virtex boxes there are two "Spartan Chips" each controlling a quarter of the total chips. These Spartan chips are FPGAs loaded with the program to retrieve the data from the chips. There is also a stripped down version of Linux running on the Virtex boxes to facilitate the communication between the DAQ computer and the Virtex boxes. Every time a spill is ejected from the PS, the Virtex box initiates data recording untill the memory is full. This takes abot 0.6 second.

Besides the chip data, the Virtex boxes also register the trigger data. Every trigger is stored as a 56 bit long number. This number contains the time stamp (24 bits), the external trigger word (10 bits), the trigger status (6 bits), and some diagnostic information like buffer overflow statuses and Spartan synchronization statuses (16 bits). To prevent too much confusion the three concepts 'trigger stream', 'trigger status' and 'trigger word' will be explained separately.

4.4.1 Trigger stream

The trigger stream is the list of different events that the system monitors as time progresses. It contains the start-trigger, framesync-triggers and the external trigger events (data triggers).

The start-trigger is the first element in the trigger stream and marks the start of the list. The system starts taking data when detecting a spill-signal. At this point the internal clock in all the connected virtex boxes is set to zero.

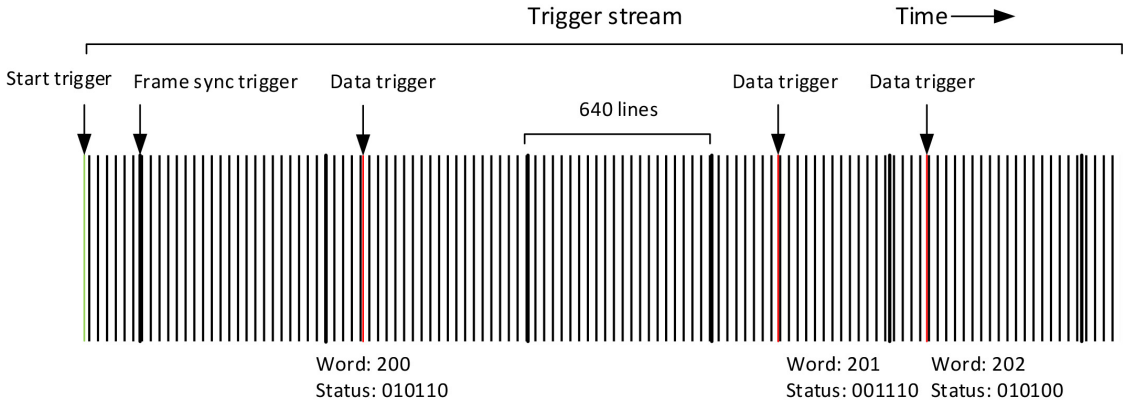

Figure 4.6: Diagram of a hypothetical trigger stream. The black bars are the frame sync triggers and the red lines the external trigger. As seen, the start trigger does not correspond to a frame sync trigger. This is also the case in the stream of the other Virtex box. This causes a significant shift between the time stamps of the frame sync triggers in the different boxes.

When the system has read out all the lines of the MAPS chips it give a signals the Virtex box that it has recorded a frame. At this moment a frame sync trigger is added to the trigger stream. This is done independently of any external trigger-event from the trigger logic (when the system is in the continuous data-taking mode as it was at both the PS and SPS beam test). The recording of the frame-sync triggers happens independently in both the Virtex boxes and thus depends on

the MAPS-chips and the PCB's that this particular box controls. Because of this, the frame sync triggers in the different trigger streams can have a significant shift between them. In the analysis stage, the software does not look at the frame-sync triggers to define a frame, but at the time the data trigger was recorded.

When the Virtex box receives a trigger event it records the trigger bits and the trigger word and puts this event in the trigger stream. This happens independently of the frame sync triggers and also separately in each Virtex box. The external trigger that is recorded separately in each Virtex box is generated by the same trigger logic, so in theory it should give the data triggers the same time stamp. There is however a difference in the time stamp that the two Virtex boxes give the same external trigger that normally increases as the trigger stream grows in length. This "drift" in the trigger counter is calculated by the software and taken into account during analysis.

4.4.2 Trigger counter and trigger word

The logic circuit is set up, via an OR gate, to give a NIM pulse when any or more of the triggers detect a particle. This signal is counted by the 'trigger word generator' and presented to the Virtex boxes as ten separate TTL signals to get a 10-bit number (from 0 to 1023). This 10-bit number that gets assigned to a specific trigger event is called the 'trigger word'. Every time the Virtex boxes receive a trigger-event they sample the signal from the trigger word generator and number the trigger event accordingly. This makes sure that all the connected Virtex boxes number their trigger events with the same number they get from this independent counter. This is later used to match the trigger events in the different Virtex boxes.

4.4.3 Trigger status and the trigger bits

Besides a trigger word, the Virtex boxes also record the triggers that fire for each event. If for example the PF-, HVF- and the C_1C_2F-trigger fire, you most likely see an electron that enters the detector in the middle. This information is of course crucial to find the frames that you are interested in for analysis. This trigger status is saved in the trigger stream as a 6-bit number.

The amount of bits that the Virtex boxes record is, in this case, limited to the logic hardware and the Virtex boxes because the they only accepts 5 external trigger inputs. At the PS and SPS beam test there were 5 bits used. The zeroth bit is generated internally by the Virtex boxes and is called the frame sync status bit. This bit is 0 when the trigger is an external trigger and 1 when it is a frame sync trigger.

Table 4.1: Bit satus corresponding to a certain external trigger and the input on the electronics used at the PS beam test.

Bit name	Bit position	Electronic input
Frame sync	100000	internal
C_1C_2F	010000	5
BF	001000	4
PF	000100	3
HVF	000010	2
Spill	000001	1

4.5 Analysis Software

The analysis software is based on ROOT. This is a C++ extension developed by CERN full of libraries for making histograms and handling large data sets. The data that is recorded first has to be demultiplexed. This process reorders the data into a data format that ROOT can work with efficiently.

When a particular spill is analysed by the software first loads the demultiplexed data and the trigger streams from both the Virtex boxes and stores them in the memory. It also loads the background (pedestal) measurements that are made every few hours. It then uses the trigger stream to find the parts of the data with external triggers in it. When it gets to a trigger it matches this trigger with the proper trigger of the other trigger stream using the trigger word, the trigger status and the time stamp. When a matching trigger is found the software constructs a frame as seen in figure 4.7. This frame contains the data from all the 24 layers.

4.5.1 Past-future protection

When two or more triggers are close to each other it could mean that more than one particles were in the detector. This effect is called "saturation". The detector cannot distinguish between two different particles when their tracks or showers overlap. For this reason the frames with a trigger overlap are omitted from the data by the past-future protection. "Past-future" because either a trigger - before or after - that causes an overlap can mean that the detector is saturated for that frame. Frames that fail the past-future correction are called "collision frames" and they are omitted from the analysed data.

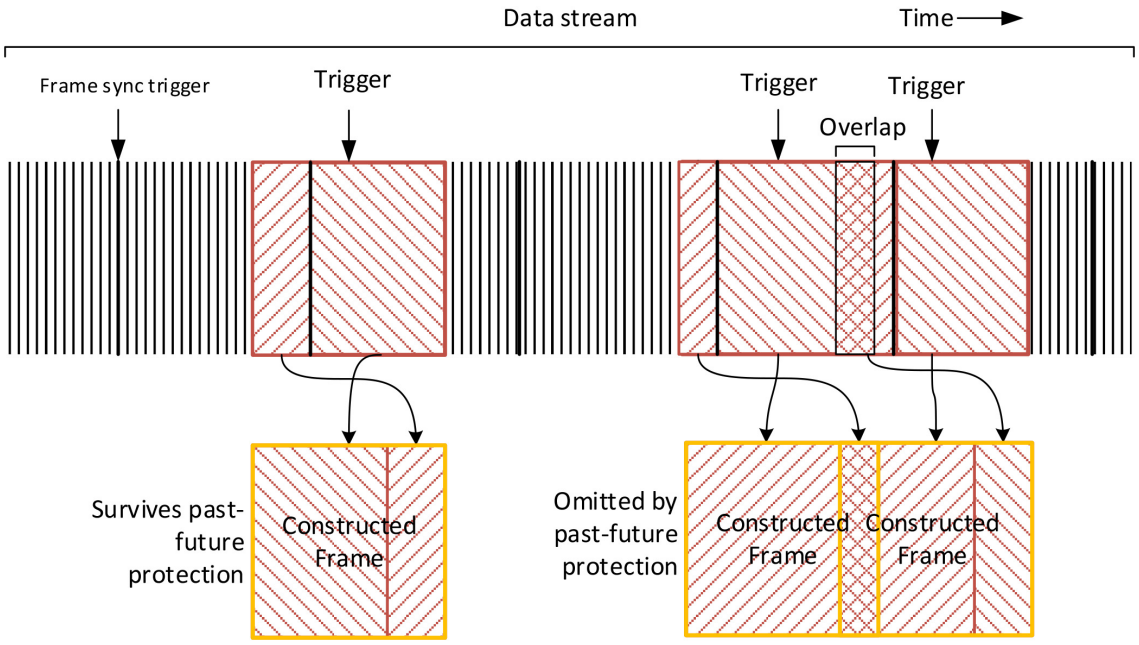

Figure 4.7: The process of making a frame. In this diagram the first frame would be usable and the second and third frame would be discarded because of the chance of saturation.

Chapter 5

The trigger system

5.1 What is triggering

In the field of subatomic physics you often have to cope with huge amounts of data, but not all of this data has useful information inside of it. When it takes a lot of time and resources to ship, analyse and store these amounts of data it is very useful to make a selection of what data to keep and what data to throw away beforehand. High resolution detectors such as the MAPS-chips generate a lot of data but cannot discriminate between a frame with a particle in it or an empty frame. Either way it stores the frame in the memory and copies it to the DAQ machine. The use of high speed detectors, such as scintillators and Cherenkov detectors, can tell the system if a certain frame contains a particle that the researchers are interested in. The system then only ships out the interesting frames that contain useful information.

At the beam test done at the Proton Synchrotron the system did not wait for a trigger to ship out the data, but filled the memory in about half a second of continuous data taking. This was done to collect as much data for analysis and debugging as possible. However, the triggers were still recorded by the system and are of great importance when the data is analysed.

5.2 Broken cables and reconstructing the trigger counter

During the PS beamtest there was a unfortunate accident where the flat cable connects the trigger counter from the trigger logic (located in the control room) with the virtex boxes (located in the test area) was damaged. Four of the flat cables' sub-wires that conveyed the least significant trigger bits were lost. This means that the 10 bit long trigger word for this data always starts with four zeros. Because the software matches the triggers from both virtex boxes by trigger word and trigger status, this broken cable causes the software to throw away fifteen out of sixteen triggers that were recorded. This greatly reduces the amount of data that is actually used for analysis. The broken flat cable does not affect the actual pixel data so this information was recorded correctly by the Virtex boxes.

Because only the four least significant bits in the trigger word were lost, the recorded trigger counter has a consistent pattern, as seen in table 5.1. This consistency makes correcting the trigger counter straightforward. This is the case because it is possible to correct it using only the trigger stream from the Virtex box with the broken trigger cable.

Table 5.1: The first column shows the trigger word bits generated by the trigger logic, the second column the trigger word bits that are received by the Virtex boxes (with the four least significant bits missing due to the broken flat cable) and the third column the resulting trigger word in decimal notation. The last column shows the correction value that need to be added to the trigger word to properly repair the trigger stream.

Trigger word made	Trigger word received	Decimal	Correction
0001101101	0001100000	96	13
0001101110	0001100000	96	14
0001101111	0001100000	96	15
0001110000	0001110000	112	0
0001110001	0001110000	112	1
0001110010	0001110000	112	2
0001110011	0001110000	112	3
0001110100	0001110000	112	4
0001110101	0001110000	112	5
0001110110	0001110000	112	6
0001110111	0001110000	112	7
0001111000	0001110000	112	8
0001111001	0001110000	112	9
0001111010	0001110000	112	10
0001111011	0001110000	112	11
0001111100	0001110000	112	12
0001111101	0001110000	112	13
0001111110	0001110000	112	14
0001111111	0001110000	112	15
0010000000	0010000000	128	0
0010000001	0010000000	128	1
0010000010	0010000000	128	2

5.2.1 Calculating the correction values

The correction is done when the software loads the trigger stream of one spill into the memory. It is not possible to determine the correct trigger word by looking at the trigger itself, it needs the context of the trigger stream that it is embedded in. The correction algorithm goes through all the triggers in the stream and every time it loads a data trigger it raises the correction value by 1. It also looks at the previous data trigger and when the broken trigger word is changed the correction value is reset to zero. For example for the trigger stream in table 5.1, this would be when the trigger word that is received jumps from 0001100000 (96) to 0001110000 (112) and when it jumps from 0001110000 (112) to 0010000000 (128).

In some rare cases an external trigger is not recorded. This can result in a maximum of 15 triggers with wrong trigger words. When there is a jump in the original trigger counter the correction is still reset to zero, so this problem does not propagate through the rest of the trigger stream.

5.2.2 Defining the initial correction value

The first data trigger in the broken trigger stream is not necessarily the same as in the correct trigger stream. Therefor an initial correction value needs to be calculated at the beginning of every spill. In the trigger stream in table 5.1 the initial correction value should be 13. To calculate this value the broken trigger words of the first twenty data triggers are stored in a list. Then the position where there is a jump in the trigger word (the first jump) is determined. (In this case this would be the third position.) Then the initial correction value is the multiplicity of the broken bits (in this case 4 bits, so a multiplicity of 16) minus the position of the first jump in the trigger counter.

5.3 Ghost triggers; improving the amount of frames analysed

During the reconstruction of the broken trigger streams a different problem with the recording of the triggers was found. This problem was not solely found in the broken trigger streams , but also in the data recorded during different beam tests and in the PS data before the cable was damaged (see table 5.3 for specific beam tests and runs). The problem manifests itself as two rapidly succeeding data triggers in either one of the trigger streams of the different Virtex boxes. A typical case is shown in table 5.2. Here you can see two trigger streams from the two Virtex boxes for the same run and spill. The data triggers in the two boxes fall roughly on the same Virtex clock tick, with a shift of 7 clock ticks (700ns) that drifts to 8 clock ticks between entry 495 and 499.

The interesting triggers in these two trigger streams are the ones at entry 495 and 496. These triggers are the double triggers referred to as 'ghost triggers', opposite the single triggers referred to as 'normal triggers'. A few characteristics can be seen in this example that hold for the other ghost triggers as well.

- The two triggers are rapidly succeeding one another, in this case 1 clock tick.
- The two triggers have the same trigger word.
- The two triggers have a different trigger status and neither one of them matches with the trigger status in the other Virtex box.

Table 5.2: Two trigger streams from both Virtex boxes for run 220, spill 5 and entries 470 - 501. The ghost trigger discussed in this section is marked gray. The columns show, in order, the entries, trigger type, Virtex time stamp (in ticks, so one unit represents 100 ns), trigger word and trigger status. Data triggers are the external triggers form the trigger logic and "FS" stands for frame sync trigger. Note that the trigger counter from virtex box 0 has been repaired using the updated code.

	Virtex 0				Virtex 1			
Entry	Type	Time stamp	Word	Status	Type	Time stamp	Word	Status
470	FS	2790629			FS	2788721		
471	FS	2797049			FS	2795141		
472	Data	2802873	775	010101	FS	2801561		
473	FS	2803469			Data	2802866	775	010101
474	FS	2809889			FS	2807981		
475	FS	2816309			FS	2814401		
476	FS	2822729			FS	2820821		
477	FS	2829149			FS	2827241		
478	FS	2835569			FS	2833661		
479	Data	2837088	776	000101	Data	2837081	776	000101
480	FS	2841989			FS	2840081		
481	FS	2848409			FS	2846501		
482	FS	2854829			FS	2852921		
483	FS	2861249			FS	2859341		
484	Data	2867396	777	000101	FS	2865761		
485	FS	2867669			Data	2867389	777	000101
486	FS	2874089			FS	2872181		
487	FS	2880509			FS	2878601		
488	FS	2886929			FS	2885021		
489	Data	2889351	778	000101	Data	2889344	778	000101
490	FS	2893349			FS	2891441		
491	FS	2899769			FS	2897861		
492	FS	2906189			FS	2904281		
493	FS	2912609			FS	2910701		
494	FS	2919029			FS	2917121		
495	Data	2921819	779	000101	Data	2921812	779	001101
496	Data	2921820	779	001001	FS	2923541		
497	FS	2925449			FS	2929961		
498	FS	2931869			FS	2936381		
499	Data	2937008	780	000101	Data	2937000	780	000101
500	FS	2938289			FS	2942801		
501	FS	2944709			FS	2949221		

There can be two possible explanations for these ghost triggers. Either there are two particles going through the detector quickly after each other and the trigger logic or the Virtex box can't keep up with these rapidly succeeding particles, or there is only one particle going through the detector but the trigger logic or Virtex box somehow makes two triggers out of it. In the first case, the detector would be saturated during that particular frame, so the frame should not be used for analysis. In the second case the Virtex box or trigger logic separated a trigger into two parts with different trigger statuses. If that is happening, the frames with the ghost triggers should be included in the analysis.

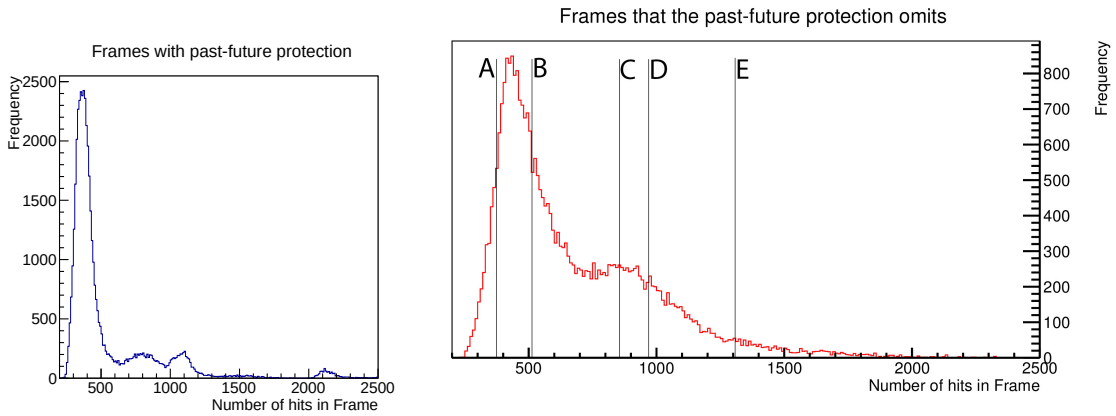

(a) **(b)**

Figure 5.1: Two histograms where the amount of hits in a frame is counted. (a) Frames with only one trigger present, so the detector is not saturated. (b) Frames with multiple (at least two) triggers in one frame, so the detector is saturated. The histogram is made from the 2 GeV/*c* data measured at the PS beam test. The bin size is set at 20.

In figure 5.1 all the 2 GeV/*c* data with and without collisions are put into a histogram to show the difference between the two. These histograms contain all the 2 GeV/*c* runs after run 150. (When the trigger logic as described in 4.3 was set up.) If there are more particles going through the detector, you would expect to see more hits in a frame. There is a considerable number of noise pixels present in the data, about 4 per chip. This should result in an average amount of noise hits of about 384 per frame. This amount will not change with multiple particles in the frame. Because certain chips don't give a signal at all, this number is lower in reality. In a detector where every chip is working and every chip gives the same cluster size a track should give approximately the same amount of hits every time (if it goes trough the whole detector). This distribution is considerably wider in the focal prototype because tracks can go through different chips that give different amounts of hits or they can go through chips that don't work at all. Tracks give in the order of 100 hits.

As expected, the frames with more than one particle (figure 5.1 (b)) in it have a peak at a higher number of hits. The frames with multiple particles (figure 5.1 (b)) shows a peak at 435 hits per frame , as opposed to the frames with only one particle in it (figure 5.1 (a)), where the peak lies around 375 hits per frame.

The difference between the peaks is not a whole track because the second track can also

partly overlap with a frame. Not only tracks can overlap. It is also possible for a track and a shower to overlap, or two showers. When there is a track in the analysed frame, and there is shower overlapping it is possible to find the range of hits between one track and a track plus a shower. These kind of overlaps contribute to the large tail of the main peak in the hit distribution of figure 5.1 (b). When there is a shower in the analysed frame and a track is overlapping, the resulting amount of hits will be between the shower hits and the shower hits plus the track hits. These overlaps contribute to the tail of the shower peak in figure 5.1 (b). It is also possible for two showers to overlap. The amount of hits will lie between one and two showers and also contributes to the shower peaks tail, but to even greater extend as the other overlap.

Looking at the peak position and the tail of the Ghost trigger distribution in figure 5.2, it seems that there are no multiple particles in the these frames. This is seen more clearly in figure 5.3 where the normal trigger distribution and the ghost trigger distribution are plotted together. The statistics for the ghost triggers are unfortunately very low because only about 2.5 percent of all the triggers are ghost triggers. This causes the amount of entries to be low.

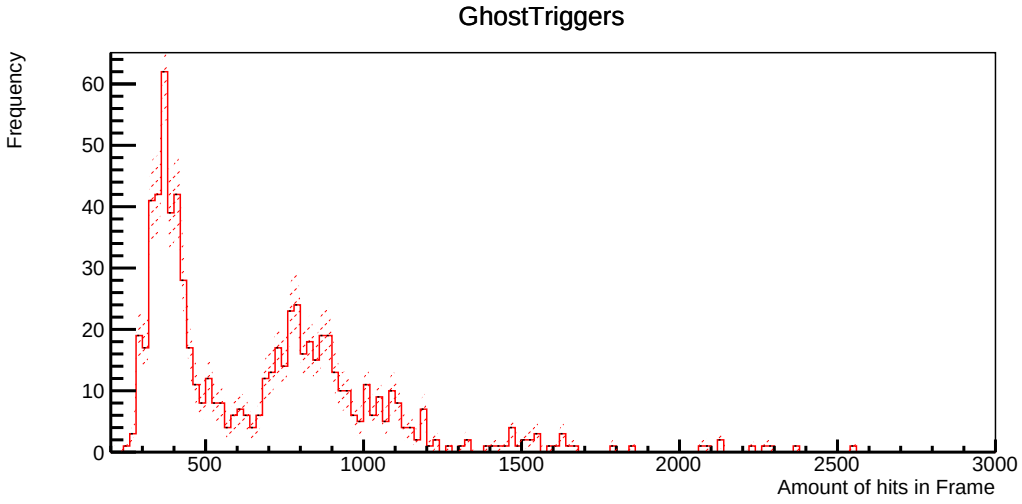

Figure 5.2: The Ghost triggers taken from 2c GeV data. Past-future protection is on and no trigger statuses are filtered. The bin size is set to 20 and the uncertainties are displayed.

5.3.1 Merging the ghost triggers

If the ghost triggers would be caused by the system interpreting a single trigger as two separate ones, the best course of action would be merging the two triggers. This way the trigger status matches with the corresponding trigger in the other Virtex box and the software can make a frame around this trigger. The procedure to merge the triggers is very straightforward. When a second trigger lies within a certain time interval from the first trigger and the two trigger words are the same, the two trigger statuses can be merged by Boolean addition. It seems logical to adopt the first trigger's time stamp and this also matches with the drift in the difference between the Virtex clocks in the different boxes that was discussed before. At last the ghost trigger trigger is deleted and only one trigger remains that the software can match with the appropriate trigger in the other trigger stream.

For the data taken at the PS beam test, comparing the trigger word is not possible because

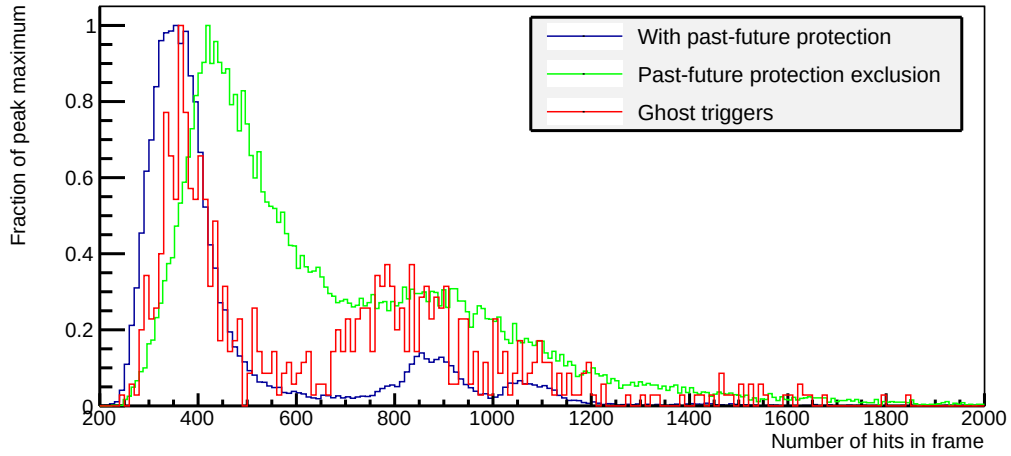

Figure 5.3: Both the histogram for the normal triggers, the ghost triggers and the frames with multiple triggers plotted together. The Y axis is that of the normal triggers. The momentum is 2 GeVc and the bin size is set at 20. In these three histograms only 2 GeVc data with the correct trigger logic setup is used (after run 150).

of the broken trigger streams in Virtex box 0. Here the ghost triggers can be identified solely by the time separation and the bit status. This means it is important to find a margin where you don't delete separate triggers that were recorded quickly after each other, but you don't leave ghost triggers in the stream. Deleting supposed ghost triggers in the stream of Virtex box 1 leads to frames with multiple particles in it that does not get filtered by the collision detection. Deleting ghost triggers in the stream of Virtex box 0 leads to malfunctions in the trigger word correction. Not deleting ghost trigger leads to less valid frames and can also cause malfunctions in the trigger word correction. In table 5.3 the percentage of ghost triggers for different margins are displayed. A margin of 1 means that the time stamp difference between the two triggers can be no greater than 100ns (one clock tick). Increasing the margin does not drastically increase the amount of triggers that are merged (maximum around 1%) so the analysis is done with a margin of 1 to decrease the chance of inappropriately merging two separate triggers.

Table 5.3: The percentage of ghost triggers present in the specified data. The margins for th PS runs is varied to study its effect. For identification of ghost triggers in the PS data, only the time difference can be used.

Beam test	Runs	Virtex	Trigger total	ghost triggers	percentage
Margin is 1					
PS	143-430	V0	218679	5304	2.46%
		V1	218305	5000	2.29%
SPS	30-256	V0	440420	3677	0.83%
		V1	441035	4116	0.93%
DESY	2-168	V0	119782	3766	3.14%
		V1	119790	3701	3.10%
Margin is 2					
PS	143-430	V0	218679	5351	2.44%
		V1	218305	5005	2.29%
Margin is 3					
PS	143-430	V0	218679	5418	2.48%
		V1	218305	5053	2.32%

Chapter 6

Data quality and hadronic shower analysis

In this chapter the data measured at the PS beam test is analysed and checked for shower patterns. The 8 GeV/c and 10 GeV/c data was measured primarily to study the hadronic shower production of protons and pions. It was hoped that there would be sufficient data to study the difference between the shower production of these particles. The data is analysed using the software made by Martijn Reicher and the trigger stream from virtex box 0 is repaired using the method described in chapter 5.

6.1 Shower containment

By using the theoretical background about hadronic showers in section 2.2.2 and table 3.2 it is possible to make some predictions about the showers that are expected to occur. Using the energies 8 GeV and 10 GeV in combination with equation 2.3 and 2.4 the shower maximum and shower depth in units of 'detector length' is obtained. The results are seen in table 6.1. With the values from table 6.1 it is not expected to see fully developed hadronic showers at the measured energies. The values do suggest that the shower maximum of both the pions and protons at both energies lie in the detector. For both energies and particles it seems like the shower maximum lies between layers 23 and 24.

Table 6.1: Rough estimates using data from table 3.2 and formula 2.3 for the shower maximum and the shower depth using formula 2.4. The values are in "shower maximum/depth per detector length" up to a specific layer. It gives the fraction of the detector needed to reach the maximum (or 95% containment) point. A value greater then 1 thus means that it does not fit in the detector up to a specific layer.

Energy	Up to layer	Pions		Protons	
		Maximum	Depth (95%)	Maximum	Depth (95%)
8 GeV	23	1.37	7.44	1.03	5.58
	24	0.65	3.53	0.56	3.04
	25	0.43	2.31	0.39	2.10
10 GeV	23	1.52	7.80	1.14	5.85
	24	0.72	3.70	0.62	3.19
	25	0.47	2.42	0.43	2.16

6.2 Hit distributions

6.2.1 Shower peaks

In figure 6.1 and 6.2 there are four hit distributions plotted. They are respectively hit distributions of frames with Cherenkov triggers and without Cherenkov triggers present. At the two measured energies it is possible to differentiate pions with protons using the Cherenkov detector. Using the linearity of the detector measured by Martijn Dietze [14] it is possible estimate the amount of particles produced in a shower. Using

$$\text{Hits} = (285.3 \pm 0.4) + (258.7 \pm 0.4) \times \text{Energy (GeV)} \tag{6.1}$$

to estimate the shower hit position for both the 8 GeV and 10 GeV data, 2337 and 2850 hits are found respectively. These hit numbers will only be found if the whole shower is contained in the detector. Both the hit distributions, with and without Cherenkov trigger, lack a peak around 2337 and 2850 hits. This suggests that there are no fully developed showers present in the data. Fully developed showers are difficult to capture in the detector because in terms of proton and pion interaction lengths, the detector is rather shallow. This was also predicted in section 6.1.

However, there is something happening around 1000 hits for both energies with the 10 GeV/c plot having a peak at slightly more hits per frame. It could hint at some kind of shower profile, but the position of the peak is a lot lower than expected. It could also be a artifact from the analysis or the data taking. From the hit distributions alone it is not clear which of them is the case. In section 6.3 this question is continued.

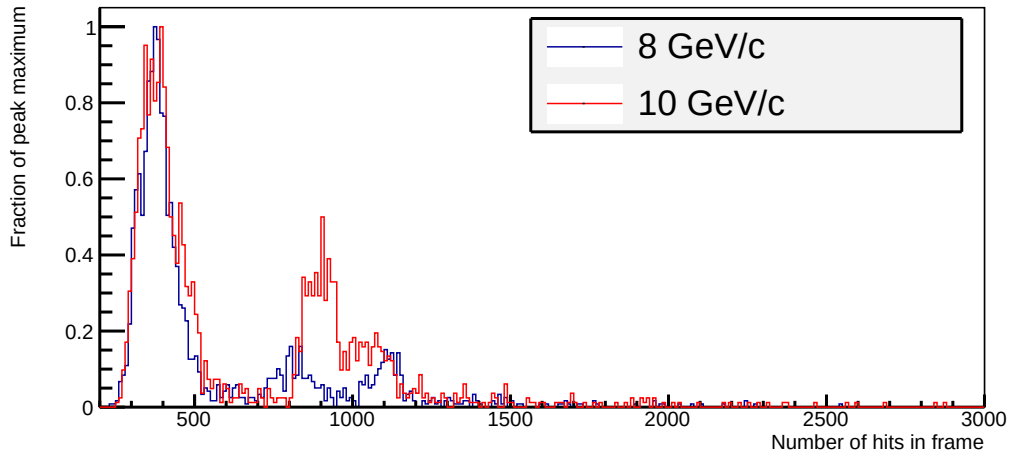

Figure 6.1: Hit distribution of frames with Cherenkov trigger. This trigger filters out the protons. The bin size is set at 20. The y-axis is normalised to the peak maximum.

Using equation 6.1 the number of hits for -2 GeVc showers is expected to be around 803. In the hit distribution of the 2 GeV/c data in figure 6.3 there is a peak at 870, which is higher than expected.

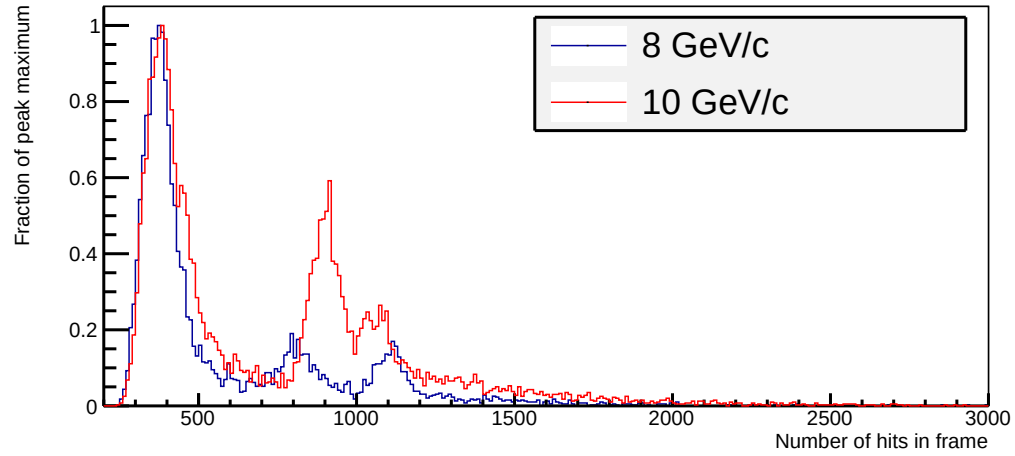

Figure 6.2: Hit distribution of frames without Cherenkov trigger. This trigger filters out the particles ligher than protons; the pions and muons The bin size is set at 20. The y-axis is normalised to the peak maximum.

6.2.2 Extra peaks

In figure 5.2 there is, for all three momenta, a second peak right from the (what looks like a) shower peak. It lies around 1200 hits for all three energies. This second peek is not according to expectations and might be a fault in the data or the analysis. At this moment it is not clear what this peak consists of and where the extra hits are coming from. This should be resolved before the data can be properly used for analysis.

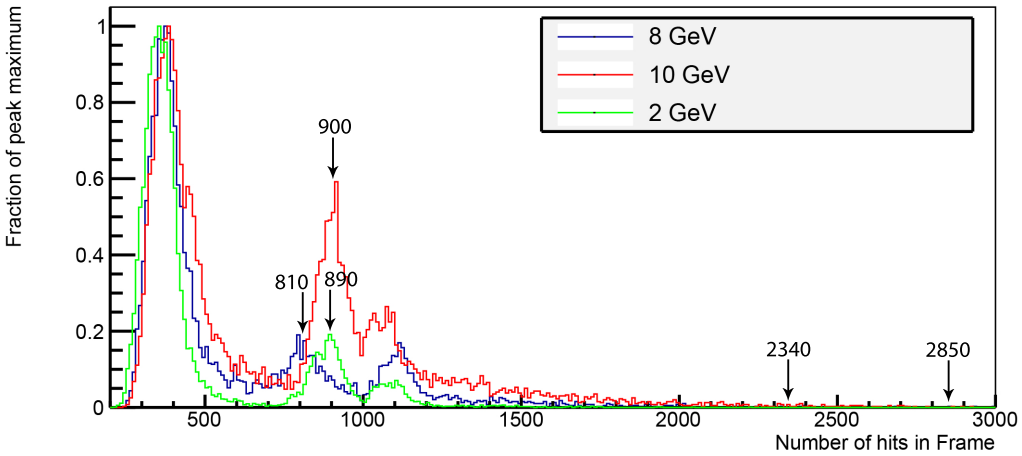

Figure 6.3: Hit distributions of three different energies without Cherenkov trigger. The data for all three energies was obtained from consecutive runs with consistent beam- and detector settings. The bin size is 10 and the Y axis is normalised to get a peak maximum of 1.

6.3 longitudinal distribution

In figure 6.4 the longitudinal distributions are plotted. These distributions show the amount of hits in each layer. There are some layers with bad chips and they give unusual high hit numbers, so that distorts the plots. In the 8 GeV/c distributions these layers are 7, 12 and 16. In the 10 GeV/c distributions these layers are 7 and 9. To enhance the shower profile, for the 8 GeV/c and 10 GeV/c data, only the frames with respectively between 700-1200 and 800-1200 hits were used. Unfortunately no clear shower profiles are visible. It was established before that the shower maximum would roughly fall between layer 23 and 24, but this is not seen in the longitudinal profiles. There is no real increase seen at all in deeper layers. This suggests that the peaks seen in figure 6.1 and 6.2 are no shower peaks but errors in data analysis or data taking. Also the plots in figure 6.5 show no clear shower profile. These plots raise even more doubt if the 8 GeV/c and 10 GeV/c data have any useful frames to compare pion and proton shower development with. The fact that the profiles in figure 6.5 have a lower hit fraction in the malfunctioning layers strengthens the idea that the peaks discussed here are not physical, but artifact in either the data analysis or the the data taking.

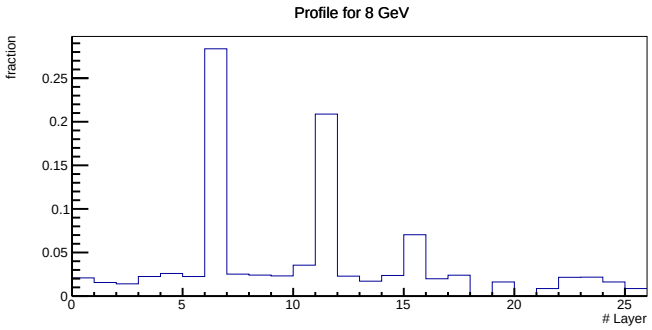

(a) 8 GeV/*c* with Cherenkov trigger

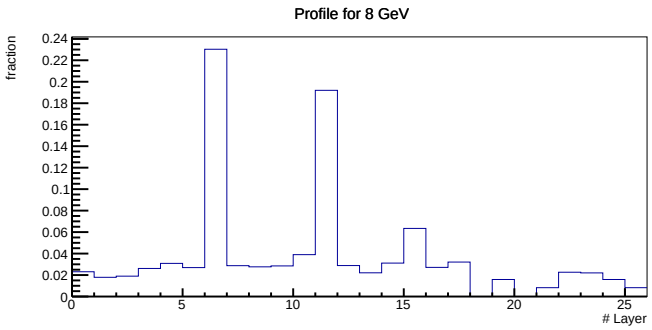

(b) 8 GeV/*c* without Cherenkov trigger

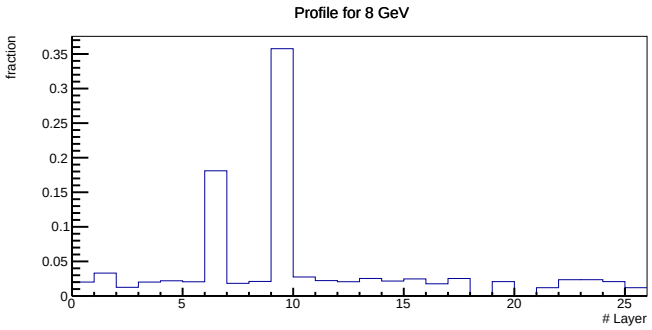

(c) 10 GeV/*c* with Cherenkov trigger

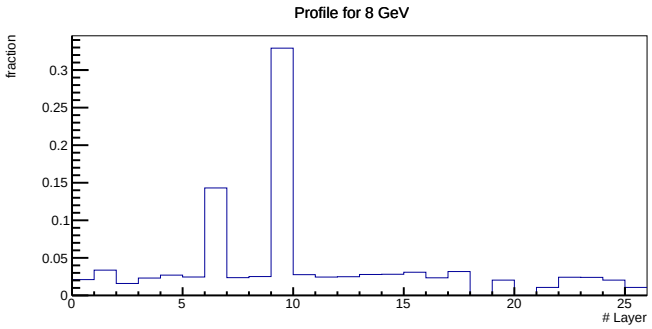

(d) 10 GeV/*c* without Cherenkov trigger

Figure 6.4: The longitudinal distributions of the 8 GeV/*c* and 10 GeV/*c* data. On the x-axis is the layer number. The layers 19 and 21 are missing thus have zero hits. The y-axis is normalised to the total number of entries in the histograms. Only the data around the peaks found in the hit distributions of figure 6.3 at 890 and 900 hits per frame were used.

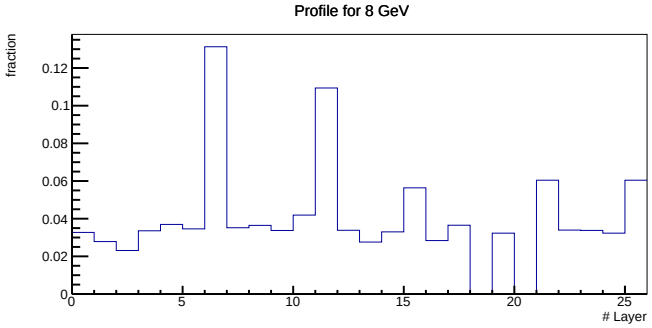

(a) 8 GeV/c with Cherenkov trigger

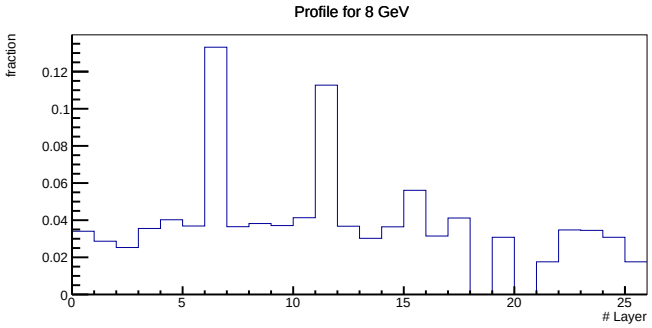

(b) 8 GeV/c without Cherenkov trigger

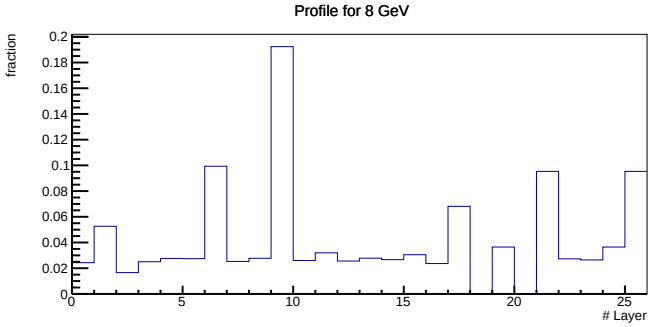

(c) 10 GeV/c with Cherenkov trigger

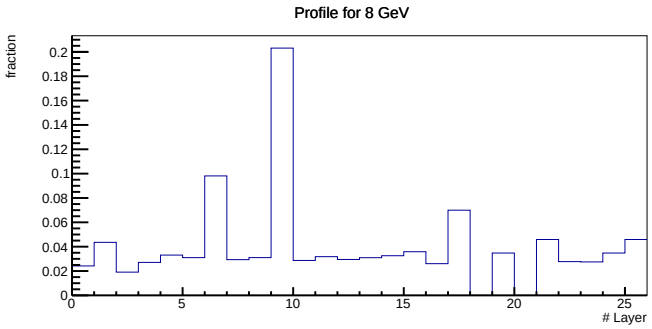

(d) 10 GeV/c without Cherenkov trigger

Figure 6.5: The longitudinal distributions of the 8 GeV/c and 10 GeV/c data. On the x-axis is the layer number. The layers 19 and 21 are missing thus have zero hits. The y-axis is normalised to the total number of entries in the histograms. All the hit numbers are included in thos profile.

6.4 Hit maps and light leaks

During the analysis of the data there was something else found that could affect the data quality. In figure 6.6 the hit maps for layer 24 and 25 are shown. It is clear that on the left side a unusual amount of hits are shown that cannot be particles. It is most likely caused by a tiny light leak. For layer 24 it would be present at the top and the left side and for layer 25 probably only at the top. If we look at the longitudinal distributions of figure 6.4 it seems like the light leak did not distort the measurement very much. This is also suggested by the hit maps because the colors stay out of the red, which indicates not more then a 10 hits maximum per pixel.

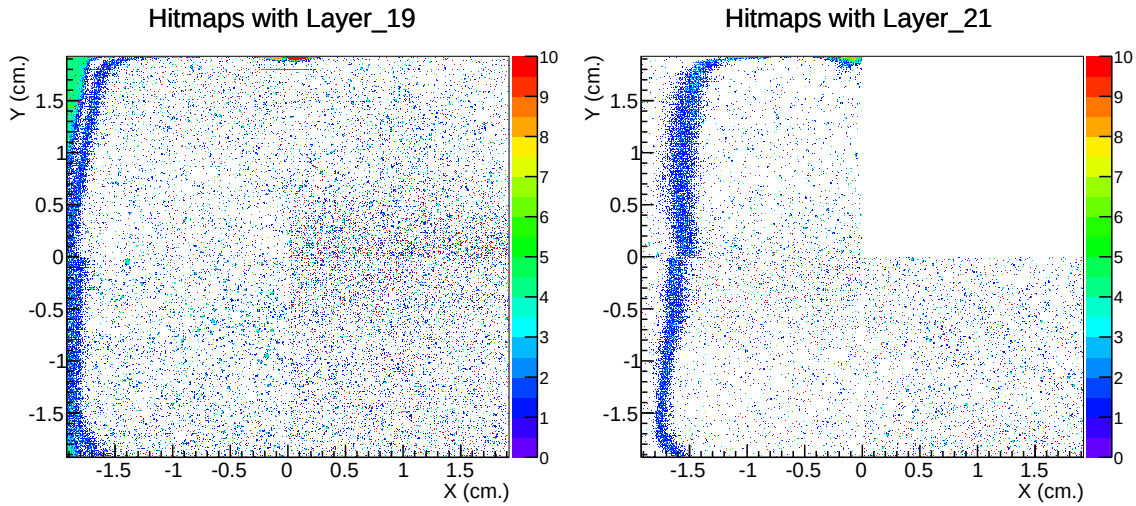

(a) Layer 24 **(b)** Layer 25

Figure 6.6: Frames of layer 24 and 25, showing the extra hits, most likely caused by a light leak. The data used comes from the 8 GeV/*c* frames without Cherenkov trigger. The x- and y-axis are in real space. The z-axis represents the amount of hits in those particular pixels for all the included runs, the magnitude is displayed with a color gradient. The software still labels these layers as 19 and 21 because layer 24 and 25 are in the Virtex box channels of these layers.

Chapter 7

Conclusions and perspectives

In this bachelor research project the trigger system was studied in detail and the data was analysed for quality checks and for studying hadronic shower production. The following conclusions and recommendations are made:

7.1 Broken trigger cable

The broken trigger cable resulted in data that could not be analysed properly. The software fix to compensate the trigger streams was implemented successfully (code can be found on the DAQ machine directory /home/jimbloemkolk/code_PS_fix). There are still some streams with problems in the analysis. This is most likely because of the fact that the ghost triggers can only be identified using the time stamp (in the PS beam test data). By setting the margin low the analysed frames are less likely to be saturated by multiple particles. It does however can sometimes cause the software fix to increase the correction value although the second trigger is a ghost trigger. This compromise sacrifices usable frames for data quality. It is not necessary to do more investigation into this trigger stream problem because the cable was repaired directly after the beam test and the chance of having the same patterns due to a damaged cable is very unlikely.

7.2 Ghost triggers

The ghost triggers seem to be normal triggers when the hit distributions of the ghost trigger frames, frames with past-future protection and the frames that past-future protection excludes are compared (see figure 5.2). There are only a few percent of ghost triggers so the statistics are low. It is unfortunately not known what the ghost triggers are caused by. It can be either in the trigger logic or the Virtex boxes. To have a complete understanding of the phenomenon it is necessary to investigate the ghost triggers better. Until this understanding is established it is safer to sacrifice a few frames and exclude the ghost triggers to improve data quality.

7.3 Data quality

The data taken at the PS beam test shows a few things that lower data quality considerably. The first thing is the light leak that affects the hadronic shower data. This effect is small so it has a minor effect on the data quality. A bigger problem for this data is the inconsistent malfunction of certain layers that manifests itself in a high number of hits for certain layers.

The extra peak next to the shower peak in the 2 GeV/c data, that is also seen in the 8 GeV/c and 10 GeV/c data, is a bigger concern. It is not known where this peak comes from and this limits the usefulness of the data considerably. Before using the beam test data for actual physics this

problem needs to be investigated and preferably fixed. It is unlikely that these peaks correspond to actual hits from particles, therefore the answer should be looked for in the data analysis or problems in the data taking or the trigger system.

7.4 Hadronic showers

With the analysis done on the hadronic showers it is not yet clear where the shower should be looked for. At 810 and 900 hits per frame for respectively 8 GeV/c and 10 GeV/c data there is a peak that might hint at some kind of showering, but the hit numbers are lower than expected. That would suggest that this peak is not caused by actual particles, but some error in the the analysis or the data taking. The longitudinal plots of this peak (figure 6.4) back up this suggestion.

Until the problem mentioned in the data quality sections are resolved and properly investigated it is difficult to conclude things about the hadronic showers. If the data can be cleaned up or is better understood the next step would be to readdress the hadronic showers.

Bibliography

[1] "Interactions of Light Charged Particles with Matter". *http://mightylib.mit.edu/Course%20Materials/22.01/Fall%202001/light%20charged%20particles.pdf*. Fall, 2001.

[2] "Bremsstrahlung defined". *https://www.nde-ed.org/EducationResources/HighSchool/Radiography/bremsstrahlung_popup.htm*.

[3] "Interactions of Heavy Charged Particles with Matter". *http://mightylib.mit.edu/course%20materials/22.01/fall%202001/heavy%20charged%20particles.pdf*. Fall, 2001.

[4] R. K. Bock, "Hadronic Shower". *http://rd11.web.cern.ch/RD11/rkb/PH14pp/node80.html*. 9 April 1998.

[5] C. W. Fabjan, "Calorimetry in high-energy physics". *http://server2.phys.uniroma1.it/DipWeb/web_disp/d6/dispense/Fabian_calorimetro.pdfl*. CERN.

[6] "The interaction of radiation with matter". *http://hyperphysics.phy-astr.gsu.edu/hbase/mod3.html*.

[7] "Electron-Positron Pair Production". *http://hyperphysics.phy-astr.gsu.edu/hbase/particles/lepton.html#c6*.

[8] SCZenz, "Schematic of a particle shower". *http://commons.wikimedia.org/wiki/File:Schematic_of_a_particle_shower.jpg*.

[9] "The Proton Synchrotron". *http://home.web.cern.ch/about/accelerators/proton-synchrotron*.

[10] G. J. Nooren, "Private communication". 2014.

[11] T. van der Brink, "Private communication". 2014.

[12] L. Pieterse, "Schematic of a scintillating crystal combined with a photomultiplier". *http://en.wikipedia.org/wiki/Scintillation_counter#mediaviewer/File:NIDetector.png*.

[13] P. Gibbs, "Is there an equivalent of the sonic boom for light". *http://math.ucr.edu/home/baez/physics/Relativity/SpeedOfLight/cherenkov.html*.

[14] M. Dietze, "Performance study of the focal prototype detector using a 2.0 - 5.4 gev pure positron beam", Bachelor's thesis, Utrecht University, 2014.